4 NEWMAN, E. H., and TEHAN, J. E.: 'Analysis of a microstrip array and feed network', *IEEE Trans.*, 1985, **AP-33**, pp. 397–403
5 JACKSON, D. R., RICHARDS, W. F., and ALI-KHAN, A.: 'Series expansions for the mutual coupling in microstrip patch arrays', *IEEE Trans.*, 1989, **AP-37**, pp. 269–274

QUANTUM WELL INTERFEROMETRIC MODULATOR MONOLITHICALLY INTEGRATED WITH 1·55 μm TUNABLE DISTRIBUTED BRAGG REFLECTOR LASER

J. E. Zucker, K. L. Jones, M. A. Newkirk, R. P. Gnall, B. I. Miller, M. G. Young, U. Koren, C. A. Burrus and B. Tell

Indexing terms: Optical modulators, Integrated optics, Semiconductor lasers, Optoelectronics

The first monolithically integrated laser/interferometric modulator is reported. The total chip length of 2·5 mm includes a 970 μm-long strained InGaAs/InGaAsP quantum well gain section, a 230 μm-long wavelength tuning section containing a distributed Bragg reflector grating, and an 800 μm-long active length Mach–Zehnder modulator based on electrorefractive InGaAsP/InP quantum wells. 4 V push–pull drive voltage produces 12·5 dB modulation depth with −9 dBm optical power coupled into a cleaved fibre.

Recent demonstrations of multigigabit ultralong-haul optical fibre transmission have employed transmitters based on Mach–Zehnder intensity modulators [1, 2]. These waveguide modulators, fabricated in titanium-diffused lithium niobate, typically have active lengths on the order of a few centimetres and are coupled to a CW laser diode optical source by means of an external fibre. Mach–Zehnder modulators fabricated from semiconductor materials hold the promise of smaller size and easier packaging because the laser can be monolithically integrated on the same substrate. Additional on-chip functionality possible for semiconductor modulators includes monolithically-integrated electronic drive, logic and control circuitry as well as monitor photodetectors.

We present the first monolithically-integrated laser/interferometric modulator. The compact chip, 2·5 mm in length, includes an $L_g = 970\,\mu m$-long gain section, a tuning section of length $L_t = 240\,\mu m$ that contains an 80 μm-long distributed Bragg reflector (DBR) grating, and a Mach–Zehnder interferometer with active length $L_{mz} = 800\,\mu m$. The waveguide layout is shown schematically in Fig. 1. The base

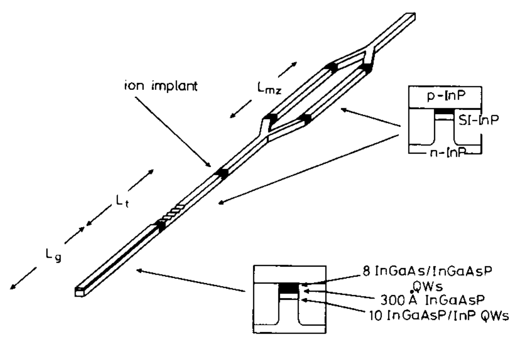

Fig. 1 *Schematic diagram of integrated DBR laser/Mach–Zehnder modulator*

$L_g = 970\,\mu m$, $L_t = 230\,\mu m$ (including 80 μm long grating), $L_{mz} = 800\,\mu m$, total length of chip is 2·5 mm
Insets show the cross-section of buried *pin* waveguide; uppermost set of eight quantum wells are 32 Å $In_{0.7}Ga_{0.3}As$/85 Å 1·25 μm composition InGaAsP; lower set are 85 Å 1·46 μm composition InGaAsP/125 Å InP; 300 Å InGaAsP layer is 1·3 μm composition

wafer structure [3] contains eight compressively strained $In_{0.7}Ga_{0.3}As$/InGaAsP quantum wells for gain in the laser section and 10 unstrained InGaAsP/InP quantum wells for electrorefraction in the modulator. For device fabrication the uppermost set of gain quantum wells are removed from the modulator and tuning sections, with the laser section protected. In the tuning section, the DBR grating is holographically defined and etched into the 300 Å thick InGaAsP cladding layer which covers the lower set of quantum wells. The continuous waveguide pattern shown in Fig. 1 is wet-etched in gain, tuning, and modulator sections with a constant rib width of ~2 μm. Finally, semi-insulating and *p*-type InP regrowths form a buried heterostructure *pin* quantum well waveguide with cross-sections in the three areas as shown in the insets to Fig. 1. Two ion implants, 200 keV H at $2 \times 10^{14}\,cm^{-2}$ dose, and 350 keV F at $2 \times 10^{13}\,cm^{-2}$ dose, provide electrical isolation between gain, tuning, and modulator sections (as well as between adjacent devices on the wafer). Top and bottom contacts are plated AuZn and AuSn. The resistance measured between the two sides of the Mach–Zehnder and between the modulator and the laser is 177 and 200 kΩ, respectively, with reverse bias breakdown on the modulator > 10 V. All measurements were performed with the device *n*-side down soldered to a copper mount held at 25°C. Both device facets are as-cleaved, and light is collected from the modulator output by means of a cleaved singlemode fibre.

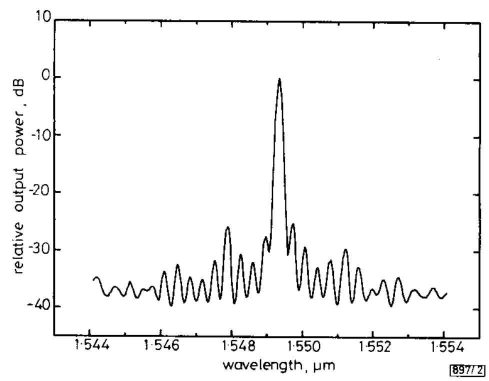

Fig. 2 *Output spectrum of integrated DBR laser/Mach–Zehnder modulator at 150 mA drive current to gain section*

Fig. 2 shows the output spectrum of the device with 150 mA current to the laser with peak wavelength at 1·5493 μm and sidemode suppression of 25 dB. The clear spectral characteristics are unchanged for all values of reverse bias to the modulator indicating sufficient electrical and optical isolation between the laser and modulator. The output wavelength is tuned by applying current or voltage to the tuning section, with a total wavelength shift of −11·4 Å for 20 mA forward bias and a shift of +13·4 Å for −11 V reverse bias. The optical output power as a function of current to the laser (with tuning and modulator sections unbiased) is shown in Fig. 3 for pulsed and CW conditions. A maximum of −9 dBm coupled into cleaved fibre is obtained.

The modulation characteristics as a function of drive voltage are shown in Fig. 4 with the laser current held constant at 210 mA. The drive voltage required for 180° phase shift when both arms of the modulator are used in push–pull configuration is $V_\pi = 4\,V$ for 12·5 dB modulation depth. To avoid forward-biasing the *pin* diode, one side of the modulator is DC-prebiased to $V_1 = -8\,V$. In this way, the two sides undergo voltage swings V_1: $-8 \rightarrow -4\,V$ and V_2: $0 \rightarrow -4\,V$. For comparison, we also show the single arm drive characteristics with a required V_π about twice that for push–pull operation. In Fig. 5 we show the modulation response as a function of drive frequency for an integrated DBR laser/Mach–Zehnder modulator with $L_{mz} = 400\,\mu m$, $L_g = 670\,\mu m$, and total chip length 1·74 mm. Electrical RF drive power of +5 dBm is applied to one side of the interferometer along with a −6 V DC bias. Laser current is 200 mA. Because the modulator has a measured series resistance of 8 Ω and capacitance of 3·3 pF, a chip 47 Ω resistor mounted in parallel with the device provides good match to the 50 Ω RF driver. We measure a 3 dB electrical modulation bandwidth of 3·14 GHz,

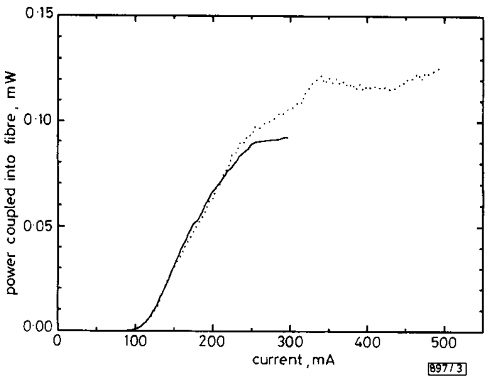

Fig. 3 *Output power coupled into cleaved fibre as function of current to gain section*

······ pulsed current conditions (obtained with 30 μs pulses at 100 Hz repetition rate)
——— CW

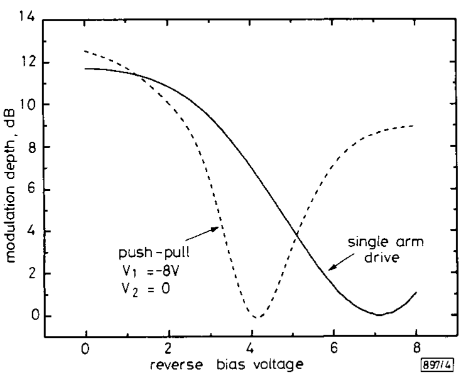

Fig. 4 *Modulation depth as CW function of drive voltage*

Current to gain section is 210 mA

in good agreement with that expected from the measured parasitics. This bandwidth is independent of the current to the gain section, indicating that there is sufficient electrical isolation between gain and modulator sections and that the electrorefractive modulator is free from saturation effects at high input optical intensity. For higher bandwidth operation, we expect to achieve significant reductions in the active length

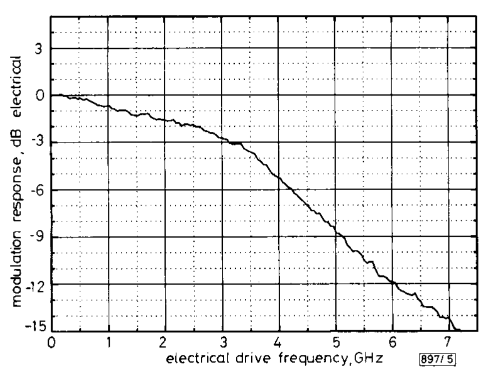

Fig. 5 *Modulation response as function of electrical drive frequency for integrated DBR/Mach-Zehnder modulator with $L_g = 670\,\mu m$, $L_t = 230\,\mu m$, $L_{mz} = 400\,\mu m$, and total chip length = 1·74 mm*

and device capacitance by increasing the number of electrorefractive QWs.

In summary, we have produced the first integrated laser/Mach–Zehnder modulator source. A compact chip, 2·5 mm in length, provides −9 dBm optical output power coupled into fibre, is wavelength-tunable about 1·55 μm for a 25 Å range, and shows 12·5 dB modulation depth for 4 V dual arm drive to the modulator. Good electrical and optical isolation characteristics between laser and modulator are provided by ion implants and an etched DBR grating, respectively. In addition, we demonstrate that the integrated device is capable of multigigahertz modulation and that the electrical bandwidths are limited only by device capacitance.

3rd August 1992

J. E. Zucker, K. L. Jones, M. A. Newkirk, R. P. Gnall, B. I. Miller, M. G. Young, U. Koren, C. A. Burrus and B. Tell (*AT&T Bell Laboratories, Room 4F-319, Holmdel, NJ 07733, USA*)

References

1 IMAI, T., MURAKAMI, M., FUKADA, Y., AIKI, M., and ITO, T.: 'Over 10,000 km straight line transmission system experiment at 2·5 Gb/s using in-line optical amplifiers'. Topical Meeting on Optical Amplifiers and their Applications, 24th–26th June 1992, Paper PD12
2 BERGANO, N. S., *et al.*: '9000 km 5 Gb/s NRZ transmission experiment using 274 erbium-doped fiber-amplifiers'. Topical Meeting on Optical Amplifiers and their Applications, 24th–26th June 1992, Paper PD11
3 ZUCKER, J. E., JONES, K. L., MILLER, B. I., YOUNG, M. G., KOREN, U., TELL, B., and BROWN-GOEBELER, K.: 'Interferometric quantum well modulators with gain', *J. Lightwave Technol.*, 1992, **LT-10**, p. 924

DIRECT DISPERSION MEASUREMENT OF HIGHLY-ERBIUM-DOPED OPTICAL AMPLIFIERS USING A LOW COHERENCE REFLECTOMETER COUPLED WITH DISPERSIVE FOURIER SPECTROSCOPY

K. Takada, T. Kitagawa, K. Hattori, M. Yamada, M. Horiguchi and R. K. Hickernell

Indexing terms: Optical amplifiers, Reflectometers, Spectroscopy, Lasers

The group delay and dispersion, including the erbium ion contributions, of the highly erbium-doped silica planar waveguide amplifier and multicomponent glass fibre amplifiers are directly measured at different pump powers using a low coherence reflectometer and dispersive Fourier spectroscopy. This method derives the refractive index spectra of these amplifiers directly from the produced reflectograms without any physical or mathematical assumptions. The dispersion of the planar waveguide amplifier at 500 mW pumping changes between +300 and −200 ps/km/nm with a 0·4 wt % erbium concentration.

Introduction: Erbium-doped fibre amplifiers are very attractive components for 1·5 μm optical fibre communication systems [1], and are finding an increasing number of applications such as in ultralong soliton systems and in soliton laser sources. The resonant gain and absorption in the doped fibres produced a strongly wavelength-dependent refractive index [2]. This dependence will lead to other optical device applications such as optical switches, which use the induced refractive index change or wavelength-dependent group delay time difference, and optical pulse compressors, which use anomalous dispersion. Only the pump-induced refractive index change at a fairly low SNR [3] and the codopant-dependent host fibre dispersion [4] have been measured, and both for amplifiers with low erbium concentrations. This Letter describes the direct measurement of the group delay and dispersion of the